Otopro Volume 22 No. 1 Nov 2026 pages. 25-36
P-ISSN: 1858-411x; E-ISSN: 2685-7863
DOI: 10.26740/otopro.v22n1.p25-36 https://journal.unesa.ac.id/index.php/jo
(This journal accommodates review, experimental, and thinking related to mechanical engineering and its application)

EFFECT OF THE CONDENSATION WATER AT THE HYDROGEN REACTOR TO IMPROVE THE FLAME CHARACTERISTICS

Sukendro Broto Sasongko [1*], *Dyah* Riandadari [2], and *Muhammad* Abdillah Akbar [3]

[1,3]Mechanical Engineering Study program, Faculty of Engineering, Adi Tama Surabaya Institute of Technology, Surabaya, 60117, Indonesia
sukendro@itats.ac.id
muhammad@itats.ac.id
[2]Mechanical Engineering Study program, Faculty of Vocation, State University of Surabaya, Surabaya, 60231, Indonesia
dyahriandadari@unesa.ac.id

Abstract. Oxyhydrogen (HHO) gas generated by water electrolysis offers a clean-burning alternative fuel with potential applicability in sustainable and distributed energy systems. This study investigates the performance of a wet-cell HHO generator operated using condensation water from a household air-conditioning system. The reactor employs iron electrodes and an electrolyte mixture containing 3 g of NaOH, with applied voltage varied between 3-24 V to evaluate its influence on gas-generation behaviour. Hydrogen evolution is quantified using an MQ-8 gas sensor. The flame propagation is captured using a high-speed digital camera (MotionPro IDT Y3-S1, 3000 fps). Flame temperature distribution is measured via a K-type thermocouple. The hydrogen dispersion downstream of the nozzle is detected by a tracer-gas analyser. Experimental results clearly show that increasing the applied voltage significantly enhances HHO production. When the voltage is raised from 5 V to 24 V, the bubble-generation increases from 0.029 to 0.341 bubbles every 60 s investigation, and the first gas bubble appears faster from 0.28 to 0.01 s. The volume rate increases from 0.104 to 2.9 mL/s. The flame widens and exhibits stronger luminosity at 24 V, consistent with higher hydrogen discharge rates and intensified combustion behaviour. The finding proposes that 70% purity condensation water produces approximately 15% greater performance compared with common water. This enhancement suggests that dissolved ions present in condensation water may improve ionic conductivity, reducing the activation resistance of the electrolysis process. The findings confirm that meaningful thermal output can be achieved using low-cost water sources, supporting the feasibility of economical HHO-based energy systems.

Keywords: Oxyhydrogen (HHO) gas; Water electrolysis; Renewable energy; Voltage variation; Wet cell generator; Hydrogen production; Energy efficiency; Flashback phenomenon; Sustainable technology.

1 Introduction

The study to reduce the using of fuel-based on fossil has excited the scholars at worldwide especially to the hydrogen energy. This persistent increase has intensified concerns regarding supply security, environmental sustainability, and dependence on fossil fuels, which remain major contributors to greenhouse gas emissions and climate instability. As countries seek to diversify energy portfolios and reduce carbon intensity, hydrogen has emerged as a key candidate for long-term decarbonisation, as confirmed by Santos and Sequeira [1] and Zeng and Zhang [2]. Indonesia reflects these global challenges. Despite possessing substantial renewable resources, the nation remains highly dependent on petroleum, natural gas, and coal. Growing population, industrial activity, and electrification continue to elevate national energy demand, highlighting the need for clean and scalable alternatives that strengthen energy security. Hydrogen produced through water electrolysis offers a promising pathway, particularly when powered by renewable electricity [2]. This finding reveals the energy from hydrogen gas. Thus, it can drive an internal combustion machine. Among available technologies, alkaline water

* Corresponding author: sukendro@itats.ac.id

electrolysis (AWE) remains the most mature. Foundational research demonstrated that activation, ohmic, and concentration losses significantly influence hydrogen-evolution efficiency [3]. Subsequent advances—including improved electrode designs and enhanced mass-transport patterns—have increased performance [4]. Rashid et al. [5] confirms that system-level modelling has further clarified electrolyser behaviour across various pressures and temperatures. Additionally, innovations in membranes, diaphragms, and electrode surface engineering have enhanced conductivity, durability, and catalytic activity [3]. Chatzichristodoulou et al. [6] findings reveal that oxyhydrogen (HHO)—a stoichiometric mixture of hydrogen and oxygen—has gained clean combustion and high flame speed. Prior studies of Appleby et al. [7] and Nanda et al. [8] indicate that HHO production increases with voltage. For Indonesia, HHO is particularly attractive when integrated with decentralised renewable systems such as solar-driven electrolysis. Experimental investigations by Burnat et al. [9] revealed that the combustion flame of HHO gas exhibits a dominant blue hue. Thus, the flame temperature of approximately 2800 °C, indicative of nearly complete combustion. Similarly, LeRoy [10] reported that the distinctive thermal and optical characteristics of HHO flames make them suitable for high-temperature applications. The chemical reactions involved in the electrolysis of water are expressed as follows (Kraglund et al. [11]). Those reactions, as presented in Equations (1)–(3), represent the cathode (reduction), anode (oxidation), and overall electrochemical reactions occurring within the system. Stojadinovic et al. [12] and Acar [13] reported a non-linear relationship between the applied voltage and gas production rate, indicating that efficiency does not increase proportionally with voltage. Similarly, the previous findings [14] found that an increase in voltage significantly enhances gas output but simultaneously raises the electrolyte temperature. Dobo and Palotas [4] reveals that the water of the fountain machine has good performance in the HHO reactor, but it is less efficient in the desert country. Because this water is only used by people for drinking, especially in countries with limited water resources. But the water from a home air conditioning system is the waste product. The condensation water still has good conductivity. So, it has potential properties for an HHO reactor. The use of iron as an electrode has been studied by Santos and Sequeira [1], who found that although iron has lower conductivity than platinum. Its significantly lower cost makes it a viable option for small-scale applications. Corrosion on iron electrodes, as described by Sharma & Singh, can be minimised by adjusting the pH and selecting the right electrolyte. The study of the low pattern of jet reveals that the flow will appear turbulent due to the hydraulic characteristic effect [7], [15], [16], [17], [18]. Thus, these ideas have been found at a common text book [19]. Previous scholars also reveal a coherent result at membrane activator at the study of hydrogen reactor [20]. However, knowledge gaps remain regarding how voltage influences flame morphology, thermal behaviour, and jet spread [9][15][16]. This study addresses these gaps by experimentally analysing voltage effects on HHO production and combustion, providing insights essential for advancing efficient and scalable hydrogen-based technologies within Indonesia's evolving energy landscape.

$$2H_2O(l)+2e^- \rightarrow H_2(g)+2OH^-(aq) \quad (1)$$

$$4OH^-(aq) \rightarrow O_2(g)+2H_2O(l)+4e^- \quad (2)$$

$$2H_2O(l) \rightarrow 2H_2(g)+O_2(g) \quad (3)$$

2 Method

Figure 1 shows the experiment stages. This flow chart shows a systematic and sequential experimental process, starting from equipment preparation, water property validation, and reactor operation under several voltage conditions, to bubble characterisation, flame, and hydrogen dispersion. Two important parameters that were validated are: DC Generator Source, operating in the range of 5–24 Volt, to ensure voltage stability during electrolysis. Physical Properties of Water (for water with 60% and 70% purity), including: Conductivity (S/cm), pH, and Total Dissolved Solids (TDS). The conductivity is ability a solution to conduct an electric current. The unit S/cm (Siemens per centimetre) is used to indicate how well a solution conducts electricity. The pH indicates the acidity level of a solution relative to the neutral value of 7. Total Dissolved Solids is the total amount of dissolved solids in a liquid, such as water. These dissolved substances can include mineral salts, metal ions, and other compounds. TDS is generally expressed in ppm (parts per million) or mg/L (milligrams per litter). For dilute aqueous solutions, 1 ppm is approximately equal to 1 mg/l. Thus, the validation ensures that the electrolyte medium has consistent characteristics before being used in the HHO production process. That is, 60% purity water is from the drinking water [2] Thus, the 70% purity water is the condensed water [2,3]. For instance, water with 60% purity exhibits a higher pH level than water with 70% purity when exposed to alkaline contaminants. After all instruments were verified, the HHO reactor was run. Observation of bubble production in the wrapping tank every 60 seconds of operation. The bubble production in the bubble wrapping tank is captured after 60 seconds of operation. The HHO reactor was then operated at several voltage levels. Those are 5, 10, 15, 18, 20, and 24 Volt. After the initial data was obtained, the next step was to analyse the bubble production rate in the bubble wrapping tank. All phenomena that appeared in each test section were observed in detail. The gas produced was then tested in a tempered glass box to see the characteristics of the flame. The final stage was to verify the dispersion of hydrogen gas coming out through the jet nozzle into the test chamber.

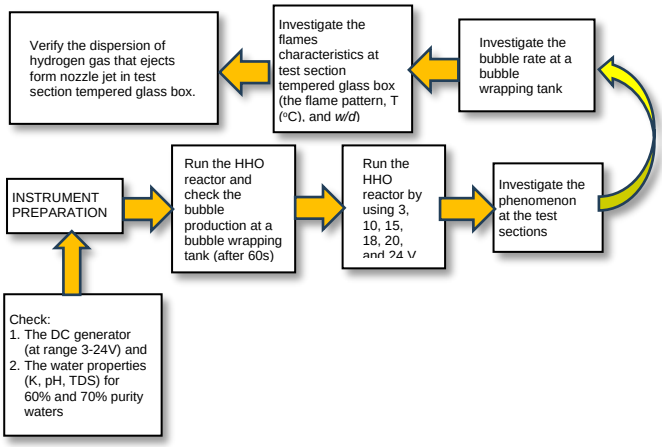


Fig. 1. The flow chart of the experiment.

Figure 2 presents the experiment setup in this study. A transparent glass reactor with dimensions 300 × 300 × 300 mm^3. It contains two iron plate electrodes with dimensions of 10 mm × 200 mm and a thickness of 2 mm. The condensation water is used as the HHO resource. It has characteristics such as conductivity 4.471×10-5 S/cm, pH 7.71, and TDS (Total Dissolved Solids) 0.5 ppm at 27 ºC. Total dissolved solids can be measured from the dissolved combined content of all inorganic substance present in a liquid in molecular, ionized, or micro-granular (colloidal sol) suspended form. The electrolysis process was driven by using a DC power generator, with voltage levels varied between 3 and 24 Volt. The electrolyte solution comprises the water with NaOH. Its composition is at 0.003 kg sodium hydroxide (NaOH) per 500 ml water. Thus, it mixed by using a 1000 mL measuring cup. A swinging spoon rotates at 10 rpm at a rotating machine to assist the mixing process. That is, NaOH acts as an activator for the conductor plates to enable the electrolysis process when they are immersed in the electrolyte solution. With a constant mass of NaOH, it is expected that a voltage effect can be observed in the hydrogen reactor. Voltage of the dimmer module ranges from 3–24 V. A square-wave form is set with 5 s. Thus, it was monitored using an oscilloscope. The flame formation from the reaction of hydrogen with oxygen was observed using a high-speed colour camera. It has a capability of 4500 fps with a resolution of 256 × 256 pixels. 80 MHz (40 MHz × 2 ch). Hydrogen bubble generation was analysed by counting the number of bubbles captured in the video recordings. Each bubble is assumed to be spherical as it passes through the outlet tube, and its volume can be calculated using Equation (4). Where V represents the bubble volume (m^3), r is the bubble radius (m), and π equals 3.14 (Çengel [19]). Equation (5), where t denotes the time of bubble rise (s) and f represents the frequency of one formation cycle (Hz). High-speed imaging analysis provides accurate measurements of bubble dynamics [9]. The volumetric flow rate indicates the total volume of gas bubbles produced per unit time (per minute), as expressed in Equation (6). A digital oscilloscope (Tektronix TBS1000 series) is deployed to ensure waveform stability for each test. A high-speed colour camera digital camera MotionPro (IDT Inc., model Y3-S1), operating at 25 frames per second, records the bubble formation and release dynamics. These image sequences are later analysed using digital image processing techniques to determine bubble frequency, size, and generation rate. The detection of hydrogen gas bubbles in the electrolysis uses an MQ-8 hydrogen gas sensor. The MQ-8 sensor employs a SnO_2-based semiconductor sensitive in the range of 100–10,000 ppm, with a typical response time of less than 10 seconds. It is monitored by a DAQ system. It is capable of recording up to 100,000 data points per second. Gas volume measurements were validated using the water displacement method, as recommended by Ehteshami et al. [16]. A Type-K (chrome–aluminium) thermocouple was employed due to its high sensitivity and operational range up to 1200 °C. The thermocouple, equipped with a 0.25 mm fine-wire bead, was mounted on a three-axis traversing stand to ensure precise positioning along the flame axis. Calibration was performed using an ice-point reference and a standard furnace, achieving an uncertainty of ±1 °C. The gas detector instrument still uses the MQ-8 sensor employs a SnO_2-based semiconductor. It can read the range of 100–10,000 ppm. It is installed with an Arduino microcontroller and a computer. By assisting the computer, the data is converted to percentage concentration in air. The maximum uncertainty of the full-scale reading of tracer-gas concentration measurement is calibrated to ±1%. Adopting 23 an L-shaped stainless-steel tube is applied as the tube of the probe for gas sampling with an outer and inner diameter of about 3 mm and 2.6 mm, respectively. The volume of a bubble of H_2 is calculated by Equation 4. The forming time of a bubble is obtained with Equation 5. Thus, capacity of the bubble generator is calculated by Equation 6.

$$V_{bubble} = \frac{4}{3}\pi r^3 \quad (4)$$

$$T_{bubble}\ (s) = \frac{1}{Frequency\ of\ a\ bubble\ cycle\ (Hz)} \quad (5)$$

$$Q_{bubble} = V \text{ x } f \quad (6)$$

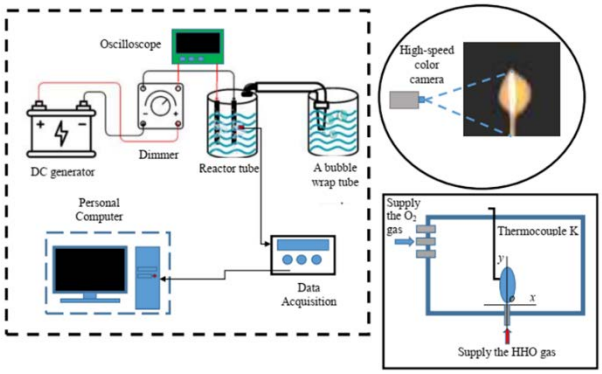


Fig. 2. The experiment setup.

3 Result and Discussion

3.1 The characteristics of the catalytic waters as a hydrogen resource

Table 1 presents the characteristics of condensation water for the 10 sample tests. The dataset contains ten samples with four measured parameters: temperature, electrical conductivity, pH, and Total Dissolved Solids (TDS). All samples were recorded at a range of temperatures of 20-56 °C. The conductivity is from 4×10^{-5} S/cm to 6.021×10^{-5} S/cm at cm-long unit, indicating extremely low ionic concentration within the electrolyte. The drinking water has a conductivity of 1.5 ×10-3 S/cm and TDS is 40 ppm [4]. The coefficient of variation is small (~3.6%), showing that the water quality is highly consistent across samples. The lowest conductivity (4×10^{-5} S/cm) suggests slightly reduced ionic mobility, while the highest value (6.021×10^{-5} S/cm) reflects marginally elevated ion presence. These variations are minimal, suggesting a stable electrolyte composition. The pH values fall within a narrow band of 7.71 to 7.79, which is slightly alkaline and characteristic of weakly buffered water. The small fluctuations (<1%) indicate consistent chemical conditions, with no significant acid–base disturbance between samples. Such uniformity suggests that dissolution of NaOH or other ionic species remained stable throughout sampling. The TDS values range between 1.21–1.41 ppm, which aligns with the very low conductivity values observed. The correlation between conductivity and TDS is evident: samples with slightly higher conductivity (e.g., Samples 5 and 7) show correspondingly elevated TDS values (1.41 and 1.40 ppm). This indicates that dissolved solids—likely sodium ions and hydroxide ions—present at trace concentrations directly influence electrical conductivity.

Table 1. The characteristics of condensed water.

Samp. No.	*T* (ºC)	Conductivity (S/cm)	*pH*	*TDS* (ppm)
1	20	3 × 10-5	7.79	1.32
2	24	4.031×10^{-5}	7.74	1.21
3	28	4.701×10^{-5}	7.74	1.30
4	32	5.037×10^{-5}	7.72	1.28
5	36	4.021×10^{-5}	7,71	1.41
6	40	5.903×10^{-5}	7.73	1.32
7	44	6×10^{-5}	7.73	1.40
8	48	6×10^{-5}	7.72	1.32
9	52	6.021×10^{-5}	7.71	1.21
10	56	6.001×10^{-5}	7.71	1.21

3.2 The production rate of gas bubbles

Table 2 presents the experimental results of the HHO reactor performance in relation to the volume of hydrogen gas generated during electrolysis. The total amount of HHO gas produced by the generator was determined from the measured volume of gas bubbles released through the outlet tube, where each bubble was assumed to be spherical in shape for calculation purposes. The experiment was performed at the voltage levels 3 to 24 Volt. It was to analyse the influence of voltage variation on gas generation efficiency. The hydrogen resource is made from the condensation water (70% purity water). The findings indicate that at 3 Volt, the electrolysis process produced only a minimal amount of gas, suggesting that the applied energy was insufficient to sustain stable bubble formation. In contrast, when the voltage was increased to 6 and 9 Volt, the rate of gas production rose significantly, and the characteristics of bubble generation became more uniform. This trend demonstrates that higher voltage improves ion mobility within the electrolyte, thereby accelerating the dissociation of water molecules into hydrogen and oxygen gases. However, the results also suggest that beyond a certain voltage threshold, further increases may not yield proportional gains in gas production due to heat build-up and energy losses. Overall, the data confirm that optimal gas production occurs within the mid- to high-voltage range, balancing efficiency, stability, and energy consumption. Based on the experimental data, it was observed that increasing the applied voltage resulted in a notable acceleration of bubble formation, as indicated by the reduction in the average time required for each bubble to form. This phenomenon occurs because higher voltage enhances the rate of electrochemical reactions at the electrode surface, thereby promoting faster dissociation of water molecules into hydrogen and oxygen gases. Consequently, the gas flow rate exhibited a clear upward trend with increasing voltage, reflecting improved ion transport and energy input to the electrolysis system. Furthermore, the total volume of gas produced per minute rose significantly at higher voltage levels, confirming that electrical energy directly influences the overall efficiency of hydrogen generation. This correlation highlights the strong dependence of HHO gas productivity on applied voltage, where optimal electrical conditions can maximise gas output while maintaining stable operation. However, it should be noted that excessive voltage may also lead to heat accumulation and reduced energy efficiency due to increased resistive losses in the electrolyte. Therefore, identifying an optimal voltage range is essential to balance gas production performance with energy utilisation and system stability.

Table 2. The hydrogen gas production

Voltage (Volt)	Volume of H_2 (ml) at a 60 s Reading	The time of first Gas Bubble appear (s)	Bubble flow rate (ml/s)
3	0.029	0.28	0.104
6	0.049	0.16	0.306
5	0.049	0.16	0.306
9	0.089	0.12	0.742
10	0.089	0.12	0.742
12	0.120	0.08	0.358
15	0.140	0.04	0.725
18	0.189	0.03	0.978
20	0.189	0.03	0.978
21	0.230	0.02	1.458
24	0.341	0.01	2.9

Table 3 illustrates the production rate of HHO gas per minute with a voltage of 24. The data were in the table illustrates the volume of hydrogen and oxygen gases produced over time at a constant voltage of 24 Volt. This finding was obtained from applying the 70% purity water. The results indicate a consistent increase in the gas volumes as the reaction time progresses, demonstrating the sustained and efficient electrolysis performance of the HHO reactor under high-voltage conditions. Initially, during the first 10 seconds, the gas production remains relatively low, with hydrogen and oxygen volumes measured at approximately 0.029–0.040 ml. This slow rate can be attributed to the system's initial stabilisation phase, where the electrolyte and electrode surfaces begin to reach optimal ionic conductivity. Beyond 15 seconds, a noticeable acceleration in gas evolution occurs, with hydrogen and oxygen volumes rising more rapidly. By 30 seconds, the generation of both gases shows a near-linear increase, indicating stable electrochemical kinetics and balanced gas output, consistent with the stoichiometric ratio of 2:1 for hydrogen to oxygen. The parallel increase in both gas types also suggests that electrode performance remains uniform throughout the test period, without signs of polarisation or gas recombination. At 55 and 60 seconds, the gas production rate increases sharply, reaching 0.290–0.342 ml for both gases. This substantial growth reflects enhanced ion mobility and reduced resistance within the electrolyte as the temperature rises slightly due to continuous electrical input. Overall, the data confirm that at 24 Volt, the electrolysis process operates efficiently, producing a proportional and stable increase in gas output over time. The consistent hydrogen-to-oxygen ratio further validates the reactors Reliability in sustaining complete water decomposition reactions, making it suitable for applications requiring stable hydrogen generation at high energy input.

Table 3. The production of gases at 1 minute and 24 Volt.

t (s)	Voltage (Volt)	Volume of gases (ml)	
		H_2 (g)	O_2 (g)
5	24	0.029	0.030
10	24	0.029	0.040
15	24	0.049	0.048
20	24	0.060	0.073
25	24	0.073	0.073
30	24	0.080	0.080
35	24	0.094	0.093
40	24	0.105	0.119
45	24	0.123	0.120
50	24	0.153	0.150
55	24	0.290	0.298
60	24	0.341	0.342

Figure 3 illustrates the relationship between voltage and the time required for bubble formation in the HHO electrolysis reactor. The graph shows a clear positive correlation between voltage and bubble-production rate, where higher voltages substantially enhance the electrolysis process. At lower voltages, such as 5 and 10 Volt, bubble formation remains minimal, indicating that the supplied energy is insufficient to overcome activation barriers—a trend consistent with the observations of Putri et al. [8] and Dobo and Palotas [4], who reported that low electrical potentials limit hydrogen evolution due to dominant activation resistance in alkaline systems. As the voltage increases beyond 10 Volt, bubble production improves significantly, reflecting more efficient dissociation of water molecules and stronger electrochemical activity at the electrode interface. This behaviour aligns closely with the findings of Zeng and Zhang [5], who demonstrated that increased voltage enhances ionic mobility and reduces polarisation effects, thereby accelerating hydrogen generation. The continued increase in bubble-production rate between 15 and 20 Volt mirrors the trends described by Chatzichristodoulou et al. [6], where elevated voltage promotes faster bubble detachment and higher current density, resulting in intensified gas evolution. The sharp rise observed at 24 Volt indicates a high-efficiency operating region of the reactor, comparable to the high-voltage performance behaviour reported by Stojadinovi et al. [12] and Burnat et al. [9], who found that hydrogen production increases steeply with voltage until thermal build-up and ohmic losses begin to limit efficiency. A

similar threshold-like behaviour was also documented in high-temperature alkaline systems studied by Kraglund et al. [11], suggesting that beyond certain voltage levels, both reaction kinetics and gas-release momentum increase dramatically before secondary thermal effects emerge. Overall, the graph confirms that applied voltage is the dominant factor controlling bubble formation in the HHO reactor, consistent with the electrochemical principles summarised by Appleby et al. [7] regarding the relationship between voltage, ion-transport mechanisms, and hydrogen-evolution efficiency. Higher voltages enhance electric-field strength and ionic mobility, directly boosting hydrogen-generation rates. However, as emphasised in previous studies, optimal operation must balance increased voltage with system stability to avoid excessive heating, energy losses, or electrode degradation. The trend observed here reinforces the broader understanding that voltage optimisation is critical for achieving high-efficiency electrolysis performance.

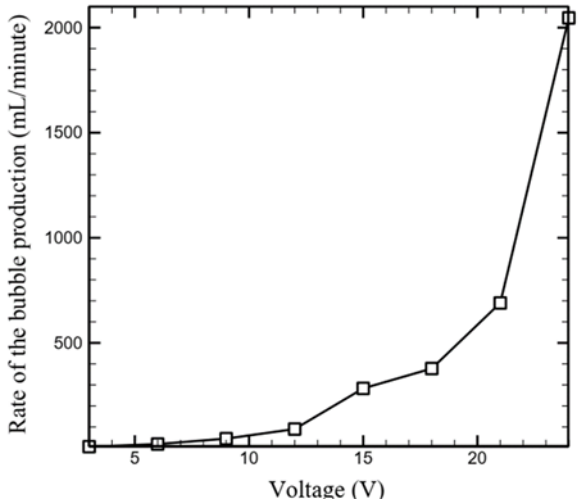


Fig. 3. Illustration of the formation time of a bubble at various voltages.

Figure 4 illustrates the time-dependent growth of gas volume during electrolysis, revealing the dynamic behaviour of hydrogen and oxygen evolution. The initial period (0–30 s), where both gases show a gradual volume increase, corresponds to the nucleation-dominated stage typically reported in early alkaline electrolysis studies. Dobo and Palotas [4] and Putri et al. [8] observed similarly slow bubble-growth kinetics at the beginning of electrolysis due to high activation resistance and limited availability of active nucleation sites on the electrode surfaces. As the process progresses beyond 40 s, the sharper rise in bubble volume aligns with the transition to a coalescence-driven regime, consistent with the intensified bubble-detachment behaviour described by Chatzichristodoulou et al. [6]. Their finding confirms that increasing current density promotes rapid bubble coalescence and accelerates the release of hydrogen and oxygen. The observation that hydrogen consistently produces larger bubble volumes than oxygen at all-time intervals also agrees with the stoichiometric ratio from water decomposition and matches the behaviour [11]. The hydrogen with higher diffusivity and lower solubility enhances its evolution rate and is relative to oxygen. The narrow initial gap between H_2 and O_2 volumes mirrors findings in high-temperature electrolysis studies [10,11]. Their study reveals attributed early-stage similarity is attributed to surface-tension constraints and limited electrode heating during the first moments of the reaction. The exponential increase observed after 50 s is also consistent with the modelling work [12]. The rising current density and local heating lower activation barriers and shift the system toward a high-efficiency operational mode. Similarly, Burnat et al. [9] documented that once electrolyte conductivity stabilises, gas evolution rates accelerate rapidly, paralleling the behaviour seen in Figure 6. The thermodynamic explanation in the present findings—where heat generation enhances ion mobility and reduces activation energy—matches the electrochemical principles summarised by Appleby et al. [7]. Overall, the time-dependent enhancement in gas evolution observed here is highly consistent with previous electrolysis research. The gradual–accelerated–exponential pattern agrees with historical alkaline, high-temperature, and modelling studies, reinforcing that bubble-growth behaviour is governed by a combination of nucleation kinetics, current density, electrode heating, and ionic transport. These similarities confirm that the HHO reactor in this study follows the established mechanistic pathways reported in prior literature while offering empirical validation under the present operating conditions.

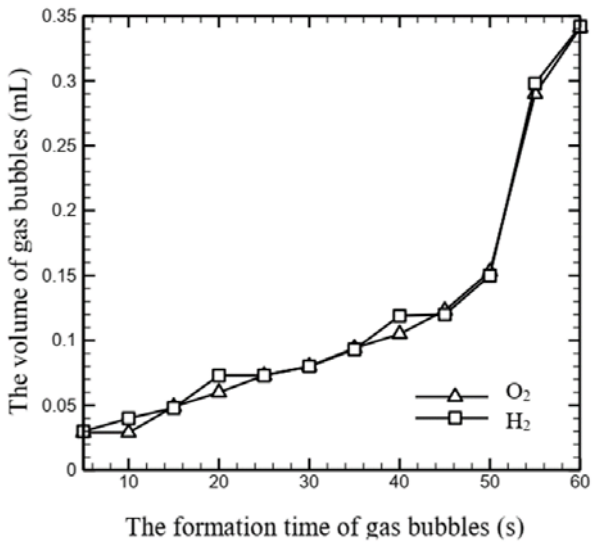


Fig. 4. The formation time of a gas bubble for Oxygen and Hydrogen at a voltage of 24 V with 70% purity water.

3.3 The current characteristics

Figure 5 compares the voltage–current characteristics obtained from two datasets: Response A from previous research (Dobo and Palotas [4]) and Response B from the present study. Both curves exhibit the typical exponential-like increase associated with

electrochemical activation and charge-transfer enhancement, yet their differences reveal changes in system efficiency. At low voltages near the onset of electrolysis (~1.9–2.0 Volt), the curves are nearly identical, though Response A shows a slightly delayed rise in current, indicating higher activation over potential. In contrast, Response B increases more promptly, suggesting reduced kinetic barriers likely due to improved electrode conditioning or a more uniform electrolyte mixture. As voltage enters the mid-range (2.2–2.5 V), Response B consistently produces higher current densities, implying enhanced charge-transport efficiency. This behaviour may result from reduced internal resistance, optimised electrode spacing, greater electrolyte conductivity, or improved bubble detachment that increases effective electrode surface area. The largest deviation occurs at higher voltages, where Response B displays a steeper current rise, indicating lower concentration polarisation and more efficient mass transport. Meanwhile, the lower current in Response A—based on Dobo and Palotas [4]—may be linked to gas accumulation, temperature variation, or less effective thermal management. Despite these differences, both curves retain similar overall shapes. The improved performance observed in Response B reflects incremental enhancements in system configuration rather than modifications to the reaction mechanism. These findings highlight the importance of optimising electrode maintenance, electrolyte preparation, and experimental control to achieve more efficient operation.

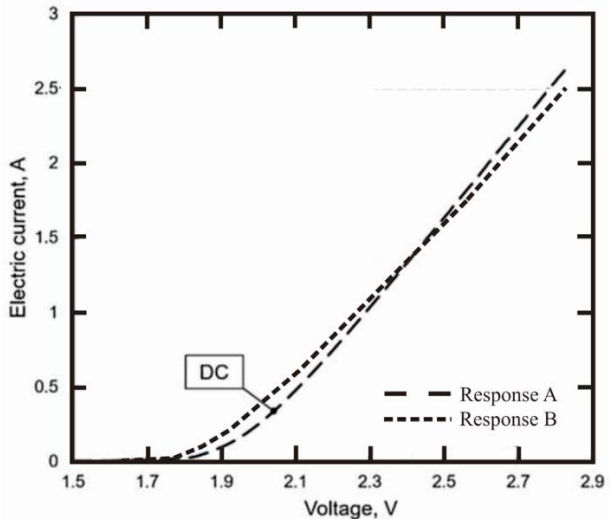


Fig. 5. Comparing previous findings with the recent study in response to the case of electric current versus voltage.

3.4 The flame characteristics

Figure 6 illustrates the morphology and intensity of the HHO flame. These visual trends are consistent with established electrolysis behaviour and prior hydrogen combustion studies. At the lowest voltage of 5 V, the flame appears as a thin, faint, vertically elongated plume. This shape indicates a limited hydrogen production rate and a low gas-discharge velocity. Figures (a), (b), (d) and (e) show that the voltages of the HHO reactor are operated at 5, 10, 15, and 20 V. Figures (c) and (f) are for operating the HHO reactor at 60% purity water and 70% purity water with 24 V, respectively. Such flame characteristics agree with early alkaline electrolysis studies, which reported that low electrical potentials are insufficient to overcome activation barriers, resulting in minimal gas evolution (Dobó and Palotás [4] and Putri et al. [8]). The pale and elongated flame at this voltage also aligns with the description by Zeng and Zhang [5]. They reveal that hydrogen generation remains constrained when ionic resistance dominates the electrochemical process. When the voltage increases to 10 V, the flame becomes wider and exhibits higher luminosity, reflecting a substantial increase in hydrogen flow rate. This behaviour aligns with the intensification mechanisms described by Chatzichristodoulou et al. [6], who found that higher voltages enhance ion mobility, accelerate bubble detachment, and produce a more stable gas flow during electrolysis. The semi-spherical flame shape observed at this stage is also consistent with hydrogen flame profiles reported in high-temperature electrolysis systems, where elevated gas-evolution rates strengthen buoyancy and broaden the combustion zone (Burnat et al. [9]). At 24 Volt, the flame reaches its most developed structure, forming a wide dome-shaped envelope with uniform luminosity. The electrolysis water of 70% pure leads at the flame performance. The flame is wider and higher. The increase of flame characteristic is about 15% larger than that in the 60% purity water. This indicates a significant rise in combustion temperature and overall reaction intensity. The trend closely matches modelling and experimental results reported by Kraglund et al. [11] and Aili et al. [20], which show that hydrogen generation increases with voltage until thermal limitations begin to reduce efficiency. The enhanced flame stability and extended curvature observed at high voltage in this study are comparable to the behaviour of hydrogen jets in high-pressure alkaline systems, where higher momentum reduces lateral diffusion and maintains a coherent flame boundary [11]. Overall, the experimental results demonstrate strong consistency with the electrochemical principles of alkaline water electrolysis and previous hydrogen combustion research—particularly regarding voltage-driven increases in hydrogen production, accelerated bubble evolution, and improved flame characteristics. These findings confirm that voltage control is the dominant factor influencing HHO production rate, combustion intensity, and flame stability in HHO-based systems.

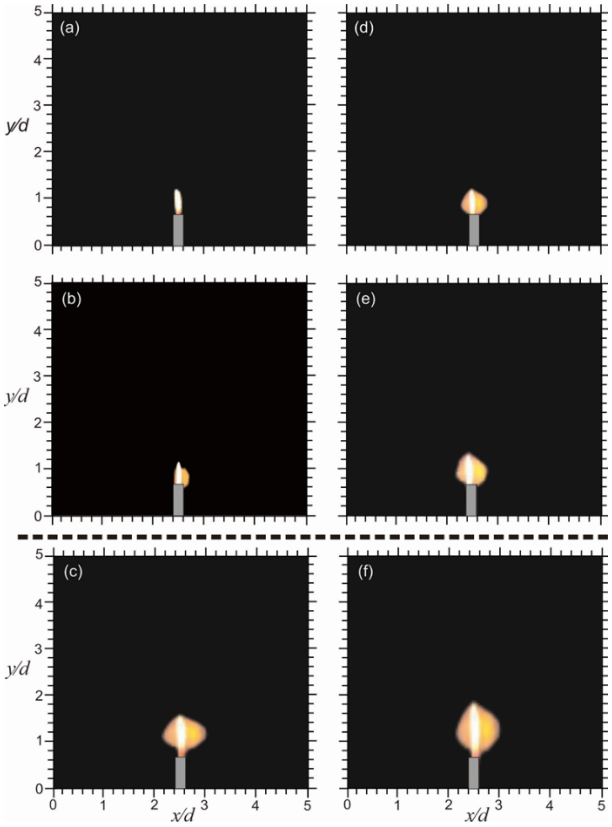


Fig. 6. Visual of flames at various voltages with the 70 % purity water. The (a), (b), (d), and (e) are the voltages of operation 5, 10. 15, and 20, respectively. The (c) and (f) are 60% purity water and 70% purity water with a voltage of 24 V, respectively.

Figure 7 presents the temperature-distribution profile in the HHO reactor as a function of the normalised position (x/d). The water has a 70% purity (the condensation water from a home air conditioning system). It is compared with 60% pure water (the drinking water). The temperature pattern exhibits clear symmetry, with a distinct peak along the central axis (x/d = 0) where the flame height is measured at y = 0.003 m under a generator voltage of 24 Volt. The maximum temperature of approximately 95 °C at the core region indicates the highest electrochemical activity and energy release. The flame produced from 70% purity water shows the highest peak temperature, reaching around 95 °C, while 60% purity water only reaches around 88 °C. This difference indicates that higher water purity increases electrolysis efficiency, resulting in a greater rate of hydrogen evolution, and thus a higher combustion intensity. This is in line with the basic trend of electrolysis, which states that contaminants in water can inhibit ion mobility and increase internal resistance, thereby reducing gas production. At each x/d position, the 70% curve consistently lies above the 60% curve, with a difference of approximately 5–8 °C in the area around $x/d = -0.5$ to 0.5. This shows that the flame from 70% purity is not only hotter, but also more stable in heat distribution. This performance indicates that the HHO gas produced is more homogeneous and free from the influence of impurity ions that can interfere with the combustion process. Both curves show temperature symmetry between the left and right sides, indicating a consistent hydrogen–oxygen mixing pattern in the flame zone. The higher water purity provides lower electrolyte viscosity and facilitates more stable bubble detachment, resulting in a more directed gas flow and a more focused flame. Water purity plays a critical role in HHO production efficiency and flame characteristics. At the same voltage (24 Volt), water with 70% purity produces a flame that is hotter, more stable, and has a more uniform temperature distribution. This shows that increasing water purity directly improves electrolysis performance and HHO flame quality.

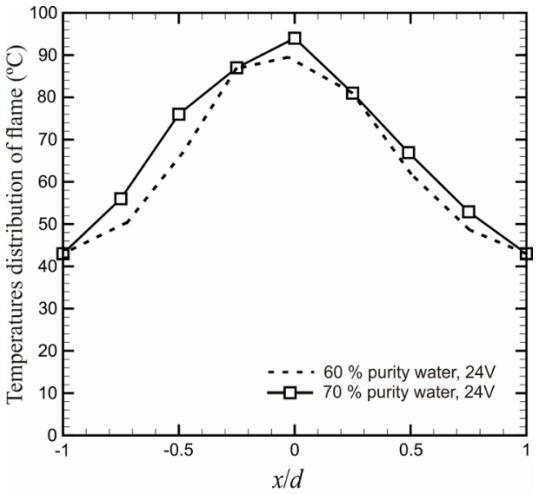


Fig. 7. The temperature distribution of the flame with the reactor voltage 24 Volt at y = 0.003 m.

Figure 8 illustrates the relationship between applied voltage and the resulting flame temperature during hydrogen combustion. The temperature distribution, measured at y = 0.005 m for several voltages (5, 10, 20, and 24 Volt), exhibits a symmetrical pattern with a clear peak at the flame centre (x/d = 0). At 5 Volt, the maximum flame temperature is approximately 65 °C, increasing steadily with voltage and reaching nearly 95 °C at 24 Volt. This positive correlation between voltage and flame temperature reflects the enhanced hydrogen-evolution rate at higher current densities. The symmetrical parabolic shape of all temperature curves mirrors earlier observations of hydrogen-flame structures in high-temperature electrolysis environments. Leroy [10] and Kraglund et al. [11] reported that hydrogen combustion at elevated gas-production rates typically produces a central high-temperature core with radial temperature decay, closely matching the pattern observed in this experiment. Similarly, the temperature rise with increasing voltage aligns with the electrochemical behaviour [5]. The increase in temperature begins to plateau at voltages above 20 Volt, indicating a saturation effect. The partial saturation in the present findings, therefore, reflects a known limitation of high-voltage electrolysis systems. Overall, the results demonstrate that hydrogen flame temperature is strongly governed by applied voltage, confirming the voltage–temperature relationship and symmetric distribution pattern described in earlier electrolysis and combustion research. The optimal 24

Volt observed here is consistent with previous studies emphasising the importance of balancing reaction intensification with thermal. The findings reinforce that careful voltage optimisation is essential for achieving stable flame structure, high thermal output, and efficient HHO-based hydrogen production.

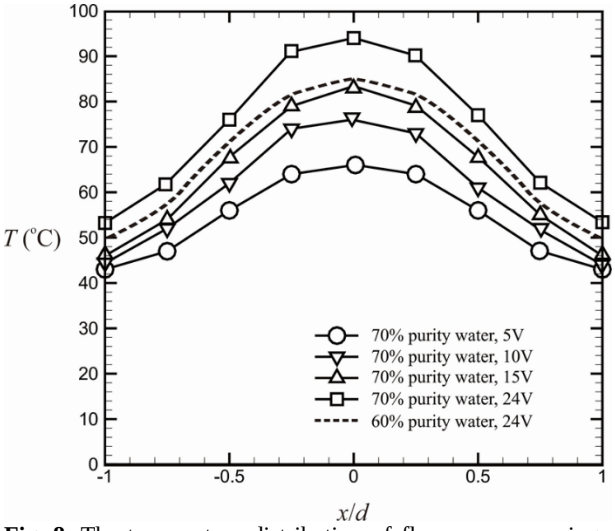


Fig. 8. The temperature distribution of flames uses varying voltages of the HHO generator at y = 0.005 m.

Figure 9 shows the variation of normalised flame width (w/d) with increasing flame height (y/d) for six applied voltages (5, 10, 15, 18, 20, and 24 Volt). The width of the flame expands progressively with height, and the degree of expansion increases significantly at higher voltages. At 5 Volt, the flame remains narrow and exhibits only modest radial growth, indicating a low hydrogen-production rate and weak discharge momentum. At 10 Volt, the flame shows a considerably larger width across the entire height range, reflecting improved hydrogen flow and stronger buoyancy forces. The higher voltage improves bubble detachment, increases current density, and enhances overall gas output. The broader flame shape is also similar to the moderate flame divergence documented [5], [7]. At 24 V, the flame reaches its maximum width, exceeding three times the burner diameter at the upper measurement region. That is, the voltage-induced acceleration of electrolysis rapidly increases gas-production rate until thermal and ohmic limitations emerge. Moreover, the strong radial divergence and elevated buoyancy at 24 Volt match the high-temperature flame behaviour. Across all voltages, the parabolic widening pattern observed is consistent with the electrochemical–thermal coupling. However, compared with previous studies, the present work demonstrates a notably sharper widening rate at high voltage, indicating stronger gas momentum relative to earlier alkaline-electrolysis configurations. This suggests that the current reactor design may facilitate more efficient hydrogen discharge, contributing to a more pronounced radial flame growth than reported in earlier literature. Overall, the results extend the findings of previous research by demonstrating that flame-width behaviour in HHO systems scales not only with voltage-driven hydrogen production but also with enhanced convective and buoyancy forces associated with higher reaction intensity. These combined effects highlight the critical role of voltage tuning in controlling flame morphology and combustion performance in compact HHO-based systems.

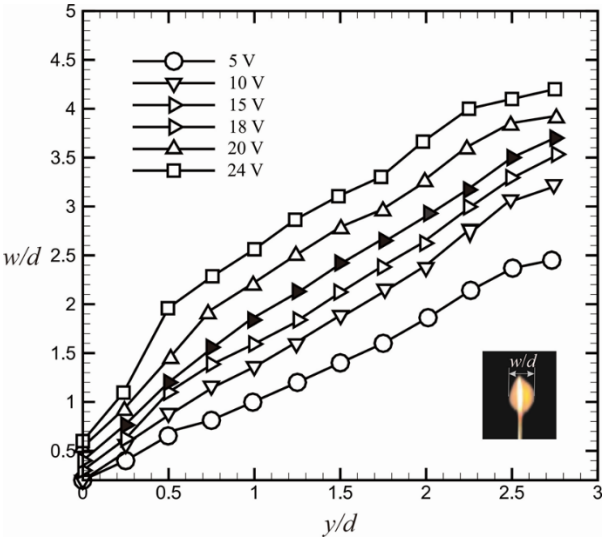


Fig. 9. The flame characteristic width at various voltages (70% purity water).

3.5 Dispersion of hydrogen gas

Figure 10 presents the variation in hydrogen dispersion at the concentration maximum (C_{max}) as a function of the normalised axial distance (y/d) at different applied voltages. This information is also compared with the data of 60% purity water. The overall trend shows a consistent decline in hydrogen concentration with increasing distance from the outlet, reflecting the expected mixing and diffusion behaviour of hydrogen in air. At lower voltages (5 and 10 Volt), the concentration begins around 75–85% near the outlet but rapidly decreases to 55–60% by y/d = 5. This steep decay is typical of low–gas-yield electrolysis conditions and aligns with the observations of Putri et al. [8] and Dobo and Palotas [4]. In contrast, at higher voltages (20 and 24 Volt), the hydrogen concentration exceeds 90% near the outlet and remains above 70% across the measured region. The improved dispersion behaviour also corresponds to the findings of Chatzichristodoulou et al. [6]. The stabilisation of the concentration profile beyond y/d = 3 suggests a transition from laminar to turbulence-assisted mixing. The hydrogen jets generated under high production rates exhibited enhanced convective transport and delayed diffusion-driven dilution, resulting in more coherent axial concentration profiles. Thus, a 70% purity water enhanced the C_{max} (the H_2 production) and led to 24 Volt. It performs the HHO reactor better than that in 60% purity water, by about 30%. The quasi-steady behaviour observed in this study closely matches these findings, indicating that higher voltages promote jet stability and directional flow formation. The saturation-like behaviour at high voltages also reflects the thermal and mass transport with a uniform pattern at downstream concentration

fields before thermal and ohmic limitations emerge. The dispersion of voltage emphasised that the operational voltage governs both electrochemical kinetics and plume dynamics in electrolytic hydrogen systems. Overall, these results confirm that applied voltage is a critical operational parameter shaping hydrogen dispersion characteristics. Higher voltages not only increase hydrogen yield but also strengthen jet momentum, reduce radial diffusion, and maintain concentration stability—behaviour consistent with prior electrolysis and hydrogen-jet studies. While improved uniformity benefits combustion stability and system efficiency, the risk of localised hydrogen accumulation highlighted in earlier literature underscores the need for careful voltage optimisation to balance productivity, dispersion control, and operational safety.

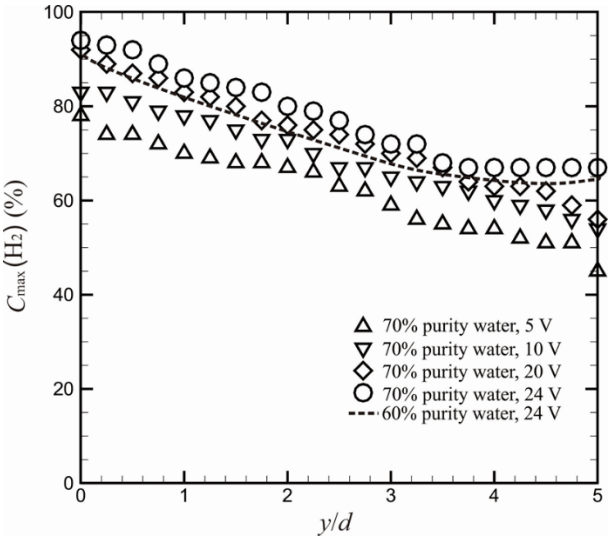


Fig. 10. Dispersion of hydrogen gas at various voltages with $x/d = 0$.

Figure 11 presents the lateral dispersion profile of hydrogen concentration as a function of the normalized position x/d for four applied voltages: 5, 10, 20, and 24 Volt. It shows the hydrogen concentration spread near downstream (y = 0.005 m). The 70% purity water performs the HHO reactor. The 60% purity water is still used as a comparison in this finding; the experimental results reveal a clear and systematic dependence of hydrogen distribution on the electrolysis driving potential, highlighting the strong coupling between hydrogen generation rate, jet momentum, and subsequent mixing behaviour in the near-field region of the nozzle. At the lowest voltage (5 Volt), the hydrogen concentration remains nearly uniform across the lateral positions, ranging between 12–14%. This relatively flat profile reflects the weak gas-evolution rate under low electrochemical driving force, resulting in a slow and diffusive jet. The low discharge momentum promotes rapid mixing with surrounding air, causing early dilution and minimizing spatial gradients in concentration. Such behaviour is consistent with earlier observations in low-current alkaline electrolysis regimes, where limited bubble nucleation and reduced jet velocity constrain the formation of coherent gas plumes. At 10 Volt, the concentration increases noticeably, reaching 20–24% near the plume centre (x/d = 0). The emergence of a mild peak indicates that higher voltage enhances the electrochemical kinetics, producing a stronger and more focused gas flow. Nonetheless, the lateral spread remains relatively wide, showing that although jet momentum increases, diffusion still plays a dominant role in shaping the concentration field. A pronounced transition occurs at 20 Volt. Here, the concentration peak approaches ~35%, and the lateral gradient becomes more distinct. This behaviour demonstrates that the intensified hydrogen-generation rate significantly increases axial jet velocity, reducing early-stage dilution and allowing the plume to maintain its coherence farther from the nozzle. The steeper profile suggests reduced entrainment of ambient air near the plume core, consistent with behaviour reported in high-voltage hydrogen-jet studies where enhanced mass flux reduces lateral dispersion. The most substantial enhancement is at 24 Volt, where the hydrogen concentration reaches-57% at the centre, gradually decreasing toward the edges. This sharp peak reflects a highly energetic and concentrated jet resulting from elevated current density and accelerated bubble coalescence in the electrolysis chamber. The strong plume momentum suppresses radial diffusion, generating a narrower and more stable concentration field. The symmetry of the curve indicates stable jet formation and minimal turbulence-induced asymmetry during operation. That is, the potential of the HHO reactor appears to be better at 24 Volt, in which it enhances that in 60% purity water.

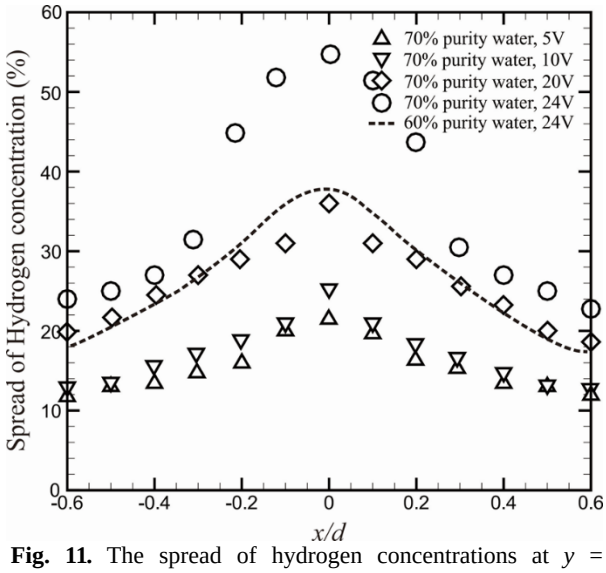


Fig. 11. The spread of hydrogen concentrations at y = 0.005m.

Conclusion

Based on the experimental results, the conclusions outlined below distil the primary technical insights obtained from this study.

1. The findings of this study demonstrate that applied voltage plays a decisive role in governing the electrochemical performance, gas-generation rate, and combustion behaviour of the HHO electrolysis system. At low voltage, the electrolyser operates

with limited ion mobility, producing sparse bubble formation, low hydrogen output, and a weak, unstable flame. As voltage increases, reaction kinetics intensify, resulting in higher bubble density, faster gas evolution, and significantly greater volumetric flow rates. This enhancement leads to stronger combustion characteristics, including increased flame height, improved luminosity, and higher core temperature.

2. Hydrogen dispersion patterns also shift with voltage, where higher voltages generate a more coherent jet with extended concentration length due to greater momentum at discharge. However, insufficient flow rates at lower voltages increase the likelihood of flame flashback, indicating that stability is closely linked to gas-ejection speed. Thermal imaging further confirms that the highest temperature region consistently aligns with the flame centreline and intensifies with increasing voltage.
3. Overall, the results highlight that voltage optimisation—not simply increasing power—is essential for achieving efficient and stable HHO production. Appropriate voltage selection can maximise hydrogen output, enhance combustion performance, and reduce operational risks, forming a strong foundation for improving small-scale hydrogen systems and their integration into cleaner energy applications.

Reference

[1] D. M. F. Santos and C. A. C. Sequeira, “Revisão,” vol. 36, no. 8, pp. 1176–1193, 2013.

[2] K. Zeng and D. Zhang, “Recent Progress in Alkaline Water Electrolysis for Hydrogen Production and Applications Recent Progress in Alkaline Water Electrolysis for Hydrogen Production and Applications,” pp. 1–112.

[3] S. S. Kumar and H. Lim, “An overview of water electrolysis technologies for green hydrogen production,” *Energy Reports*, vol. 8, pp. 13793–13813, 2022, doi: 10.1016/j.egyr.2022.10.127.

[4] Z. Dobó and Á. B. Palotás, “Impact of the current fluctuation on the efficiency of Alkaline Water Electrolysis,” *Int. J. Hydrogen Energy*, vol. 42, no. 9, pp. 5649–5656, 2017, doi: 10.1016/J.IJHYDENE.2016.11.142.

[5] M. Rashid, M. K. Al Mesfer, H. Naseem, and M. Danish, “Hydrogen Production by Water Electrolysis : A Review of Alkaline Water Electrolysis , PEM Water Electrolysis and High Temperature Water Electrolysis,” no. 3, pp. 80–93, 2015.

[6] C. Chatzichristodoulou, F. Allebrod, and M. B. Mogensen, “FOR I NCREASED High Temperature Alkaline Electrolysis Cells with Metal Foam,” vol. 163, no. 11, pp. 3036–3040, 2016, doi: 10.1149/2.0051611jes.

[7] A. J. Appleby, G. Crepy, and J. Jacquelin, “HIGH EFFICIENCY WATER ELECTROLYSIS IN ALKALINE SOLUTION,” vol. 3, pp. 21–37, 1978.

[8] N.A.Z. Putri, I. Yuliani, and S. Widarti, “Pengaruh Pemakaian Jenis Bahan Bakar Terhadap Kinerja Boiler dengan Metode Langsung dan Tidak Langsung,” *J. Surya Tek.*, vol. 11, no. 1, pp. 349–356, 2024, doi: 10.37859/jst.v11i1.7324.

[9] D. Burnat *et al.*, “Composite membranes for alkaline electrolysis based on polysulfone and mineral fi llers,” *J. Power Sources*, vol. 291, pp. 163–172, 2015, doi: 10.1016/j.jpowsour.2015.04.066.

[10] R. L. Leroy, “I n d u s t r i a l w a t e r electrolysis: present a n d f u t u r e,” vol. 8, no. 6, pp. 401–417, 1983.

[11] M. R. Kraglund, D. Aili, K. Jankova, E. Christensen, Q. Li, and J. O. Jensen, “Zero-Gap Alkaline Water Electrolysis Using Ion-Solvating Polymer Electrolyte Membranes at Reduced KOH Concentrations,” *J. Electrochem. Soc.*, vol. 163, no. 11, pp. F3125–F3131, 2016, doi: 10.1149/2.0161611JES.

[12] J. Stojadinovi, D. Wiedenmann, M. Gorbar, F. La Mantia, L. Suarez, and A. Z, “Electrochemical Characterization of Porous Diaphragms in Development for Gas Separation,” vol. 6.

[13] C. Acar, “Sustainability Evaluation of Solar Based Hydrogen Production Methods,” pp. 113–119, 2017.

[14] I. Flis-kabulska, J. Flis, Y. Sun, and T. Zakroczymski, “Electrochimica Acta Hydrogen evolution on plasma carburised nickel and effect of iron deposition from the electrolyte in alkaline water electrolysis,” *Electrochim. Acta*, vol. 167, pp. 61–68, 2015, doi: 10.1016/j.electacta.2015.03.132.

[15] H. A. Miller *et al.*, “Green hydrogen from anion exchange membrane water electrolysis: A review of recent developments in critical materials and operating conditions,” *Sustain. Energy Fuels*, vol. 4, no. 5, pp. 2114–2133, 2020, doi: 10.1039/C9SE01240K.

[16] S. M. M. Ehteshami, S. Vignesh, R. K. A. Rasheed, and S. H. Chan, “Numerical investigations on ethanol electrolysis for production of pure hydrogen from renewable sources,” *Appl. Energy*, vol. 170, pp. 388–393, 2016, doi: 10.1016/J.APENERGY.2016.03.001.

[17] S. B. Sasongko, R. F. Huang, and C. M. Hsu, “Effects of backward inclination on a pulsed jet in crossflow,” *J. Wind Eng. Ind. Aerodyn.*, vol. 214, p. 104662, 2021, doi: https://doi.org/10.1016/j.jweia.2021.104662.

[18] S. B. Sasongko, R. F. Huang, and C. M. Hsu, “Modulating flow and mixing characteristics of an inclined jet in crossflow at a large backward inclination angle by acoustic excitation,” *Int. J. Mech. Sci.*, vol. 209, p. 106708, 2021, doi: https://doi.org/10.1016/j.ijmecsci.2021.106708.

[19] B. Concepts, “Solutions Manual for Fluid Mechanics : Fundamentals and Applications by Çengel & Cimbala INTRODUCTION AND BASIC CONCEPTS,” 2006.

[20] D. Aili *et al.*, “Porous poly(perfluorosulfonic acid) membranes for alkaline water electrolysis,” *J. Memb. Sci.*, vol. 493, pp. 589–598, 2015, doi: 10.1016/J.MEMSCI.2015.06.057.